Activated carbon materials with a rich surface chemistry prepared from L-cysteine amino acid

S. Reljic, C. Cuadrado-Collados, E. Oliveira Jardim, J. Farrando-Perez, M. Martinez-Escandell, J. Silvestre-Albero*

Laboratorio de Materiales Avanzados, Departamento de Química Inorgánica-Instituto Universitario de Materiales, Universidad de Alicante, Spain

ARTICLE INFO

ABSTRACT

A series of activated carbon materials have been successfully prepared from a non-essential amino acid, such as L-cysteine. The synthesized carbons combine a widely developed porous structure (BET surface area up to 1000 m^2/g) and a rich surface chemistry (mainly oxygen, nitrogen and sulphur functionalities). These surface functional groups are relatively stable even after a high temperature thermal treatment ($O>N\sim S$). Experimental results show that these samples with a rich surface chemistry exhibit a significant improvement in their hydrophilic character. Although the role of the surface functional groups is less pronounced for the adsorption of non-polar molecules such as CO_2, CH_4 and C_2H_4, their adsorption at atmospheric pressure is to some extend conditioned by the characteristics of the adsorbent-adsorbate interactions. The synthesized carbons exhibit an excellent adsorption performance for CO_2 (up to 3 mmol/g at 0 °C). Furthermore, samples with a low activation degree exhibit molecular sieving properties with very promising CO_2/CH_4 (up to 4.5) and C_2H_4/CH_4 (up to 6) selectivity ratios. These results anticipate that non-essential amino acids are a versatile platform to obtain carbon materials combining a tailored porous structure and rich multifunctional surface chemistry and with potential application for gas adsorption/separation processes.

1. Introduction

The activated carbon global market is continuously growing (up to 3.31 million metric tons worldwide by 2021) due to the versatility of these materials in industry and municipalities for cleaning purposes. Their main application involves the removal of contaminants in water and air environments [1]. However, activated carbons are also important in the medical and pharmaceutical industry to remove contaminants in the production of drugs. Worldwide market is expected to continue growing due to the excellent performance of activated carbon materials in novel applications such as electrodes for electrochemical double layer capacitors (EDLC) and lithium ion batteries (LIBs), sensors, amongst others [2–4].

The attractiveness of activated carbon as a universal adsorbent is due to its low cost, the versatility in its production (e.g., a wide range of precursors can be used), and the possibility to design the porous structure and surface chemistry upon request. Although the porous structure has a profound impact on the performance of the activated carbons (e.g., microporous activated carbons exhibit an optimum performance for gas and energy storage [5,6]), the presence of surface functionalities, although being also important, has been less explored [7,8]. Heteroatoms such as oxygen, nitrogen, hydrogen and, to a lower extent, sulphur have been traditionally observed in carbon materials, leading to stable surface compounds. A priori, the nature and amount of these groups can modify the physicochemical characteristics of the synthesized carbons and their subsequent performance in a given application. However, the understanding of real role of these surface functionalities is not always straightforward due to the difficulty to isolate specific groups and the variety in their local environment depending on the carbon precursor, the pretreatment applied, etc [9].

Oxygen-containing surface groups are the most common functionalities present on the carbon surface and the most widely evaluated. The presence of oxygen surface groups has a promot-

* Corresponding author.
E-mail address: joaquin.silvestre@ua.es (J. Silvestre-Albero).

ing effect in a range of applications, such as adsorption of polar molecules (e.g., H_2O) [10–13], catalytic methane decomposition [14], hydrogen storage [15], etc. Contrary to oxygen, nitrogen functionalities are not formed spontaneously on carbons during their synthesis. These functionalities have to be incorporated either through post-synthesis methods (e.g., treatment with ammonia at high temperature) [16], or using nitrogen containing carbon precursors (e.g., polypyrrole) [17]. The presence of nitrogen functionalities has shown to be beneficial for processes such as CO_2 adsorption [17,18], electric double layer capacitance [19], metal-free oxygen reduction [20], etc. Although sulphur has been less explored in the literature, there are studies that confirm a promoting effect of sulphur for CO_2 adsorption [21], as cathode in Li-S batteries [22], as metal-free catalysts for hydrochlorination reactions [23], and in the removal of Hg in aqueous phase [24].

Despite these findings, the situation is more complex when different functional groups are present simultaneously in a given activated carbon. This is due to the difficulty to isolate the effect of each of these groups individually and to identify the presence of potential synergetic effects amongst them. Sanchez-Sanchez and coworkers managed to identify the concomitant role of nitrogen, oxygen and phosphorus functionalities in the adsorption of CO_2 at atmospheric pressure [25]. Through a careful XPS investigation, the authors managed to identify the specific role of each functionality, including the nature of the surface groups having a preferential role in the aforementioned process. Unfortunately, the evaluation of multi-functionalized activated carbons and potential synergetic effects is limited due to the difficulty to incorporate different functional groups on the carbon surface, either during the synthesis or through post-synthesis methods. A promising approach to reach these multi-functionalized carbons is the use of raw materials with a rich surface chemistry as carbon precursors, e.g. covalent organic condensates. For instance, Kossmann and workers synthesized C_1N_1 condensates from guanine with promising results for CO_2/N_2 separation [26]. A potential platform never evaluated in the literature is the use of non-essential amino acids (amino acids not used as food supplements). Amino acids are organic compounds that contain amino (-NH_2) and carboxyl (-COOH) functional groups, together with side chains that could contain other functional groups such as sulphur (e.g., cysteine & methionine). Taking into account that amino acids are the main component of proteins and, at the same time, proteins are the main responsible for CO_2 fixation in plants (through Rubisco enzyme), the evaluation of these platforms to synthesize carbon materials is *a priori* an appealing approach. In principle, amino acids are susceptible to condensate into complex structures ready to be converted into activated carbons after a proper activation step. However, to our knowledge there are no studies in the literature about the use of amino acids as precursors for the preparation of carbon materials with a rich multicomponent surface chemistry.

With these premises, the main goal of this manuscript is the preparation of activated carbon materials combining oxygen, nitrogen and sulphur functionalities starting from ʟ-cysteine as a raw material. ʟ- cysteine is a non-essential aminoacid produced industrially by hydrolysis of animal wastes (keratin), such as poultry feathers and hog hair, although it can also be obtained from fruits and vegetables [27]. Experimental results show that ʟ-cysteine can be successfully converted into high-surface area activated carbons. These carbons are purely micropores in nature and exhibit carbon molecular sieving properties (at least for samples with a low activation degree), while preserving a rich surface chemistry. These samples exhibit a very good performance for CO_2 and C_2H_4 adsorption at atmospheric pressure, associated with a promising CO_2/CH_4 and C_2H_4/CH_4 selectivity ratio, in the case of the carbon molecular sieves.

2. Experimental section

2.1. Preparation of the activated carbon

L-cysteine is a sulfur-containing non-essential amino acid. The molecule (L-Cysteine, 97%) was purchased from SIGMA-ALDRICH. In a first step, ʟ-Cysteine was spread in the alumina boat and thermally treated in a horizontal furnace at 700 °C for 2 h under a N_2 flow rate of 100 ml/min (heating ramp of 3 °C/min). The reaction process is a simple condensation of ʟ-cysteine, followed by carbonization under nitrogen atmosphere. After condensation/carbonization the yield was 5.4 wt.%. In the second step, the carbonized material was activated with CO_2 (100 ml/min) at a temperature of 800 °C with the heating ramp of 3 °C/min and the activation time of 1 h, 3 h, 6 h. An additional sample was prepared using 900 °C as activation temperature for 1 h. Four different cysteine-based activated carbons (CAC) were prepared and labelled CACxy00, where x = activation time and y = activation temperature. The yield achieved after the activation treatment is shown in the table 1.

2.2. Physico-chemical characterization

The porous structure of the synthesized samples was characterized using gas adsorption at cryogenic temperatures. Before the adsorption measurements, samples were submitted to an outgassing treatment at 200 °C for 4 h. N_2 adsorption measurements were performed at −196 °C in a home-built manometric system.

Field emission scanning electron microscopy (FESEM) images were obtained in a ZEISS equipment (Merlin VP compact model) equipped with an EDX microanalyzer Quantax 400 from Bruker. This equipment has a resolution of 0.8 nm at 15 kV and 1.6 nm at 1 kV. The XPS spectra were recorded in a XPS K-ALPHA Thermo Scientific. All spectra were collected using an Al-K radiation (1486.6 eV), monochromatized by a twin crystal monochromator, yielding focused X-ray spot elliptical shaped with a major axis length of 400 mm at 3 mA x 12 kV. The alpha hemispherical analyser was operated at the constant energy mode with survey scan pass energies of 200 eV to measure the whole energy band and 50 eV in a narrow scan to selectively measure the desired elements. Charge compensation was achieved with the system flood gun that provides low energy electrons and low energy argon ions from a single source. The CH_x in carbon 1 s score level was used as reference binding energy (284.6 eV). The powder samples were pressed and mounted on the sample holder and placed in the vacuum chamber. Before the spectrum recording, the samples were maintained in the analysis chamber until a residual pressure of ca. 5×10^{-7} Nm^{-2}. The peaks deconvolution was performed by a quantitative analysis calculating the integral of each peak, after subtracting the S-shaped background, and by fitting the experimental curve to a combination of Lorentzian (30%) and Gaussian (70%) model. Due to the chemical heterogeneity of the synthesized samples, XPS analysis have been performed in three different positions.

2.3. Atmospheric pressure H_2O, CO_2, CH_4 and C_2H_4 isotherms

Gas/vapour adsorption measurements at atmospheric pressure were performed in a manometric system designed and constructed by the LMA (Advanced Materials Laboratory) group, now commercialized by Quantachrome Instruments as VSTAR. Before the adsorption measurements, samples were outgassed under ultra-high vacuum conditions at 200 °C for 4 h. Isotherms were performed at 25 °C for all probes, except for CO_2 where 25 °C and 0 °C were tested.

Table 1
The yield of the samples.

SAMPLE	Activation time (h)	Activation temperature (°C)	Yield (%)
CAC1800	1	800	80
CAC3800	3	800	38
CAC6800	6	800	25
CAC1900	1	900	68
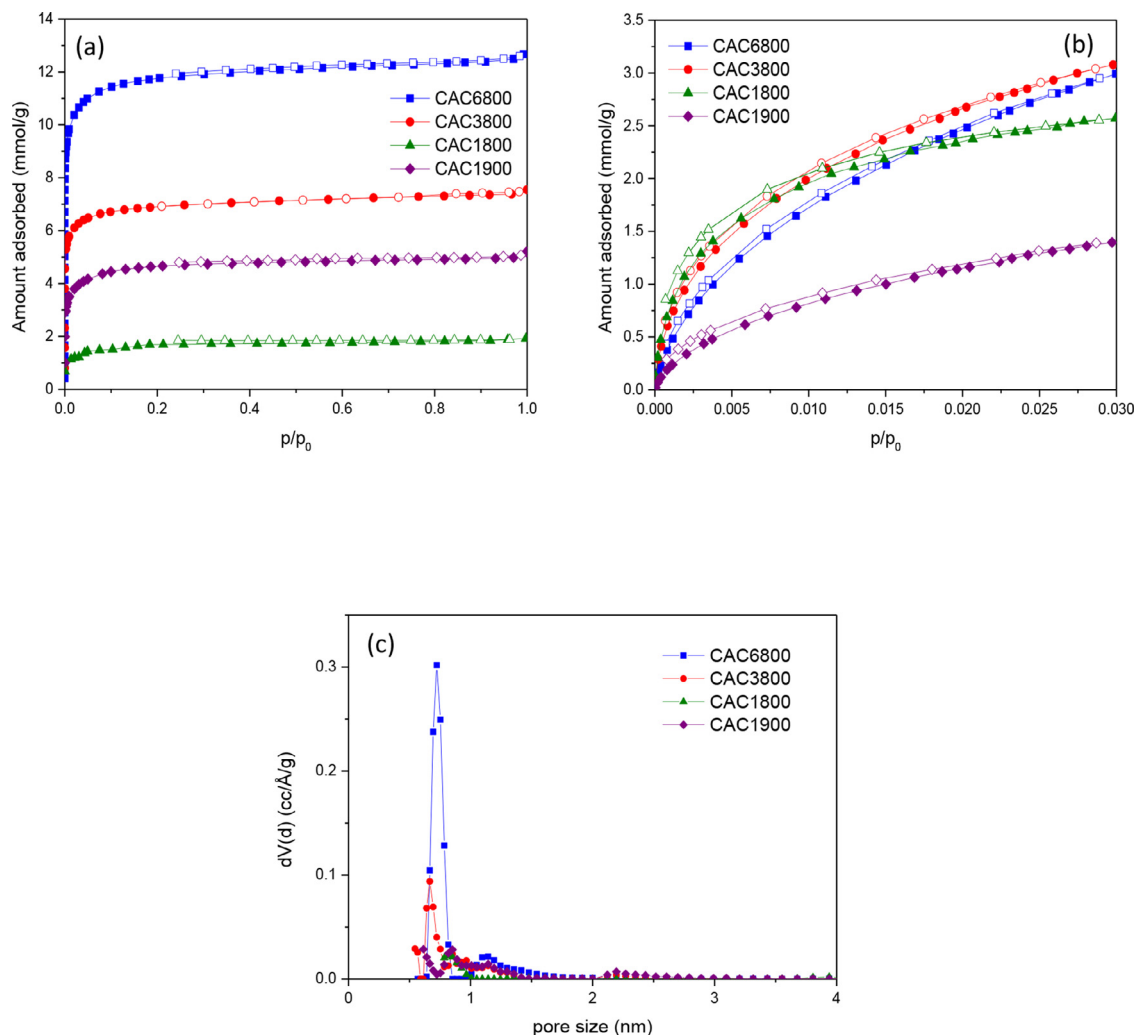
Fig 1. (a) N_2 adsorption/desorption isotherms at −196 °C, (b) CO_2 isotherms at 0 °C for the different samples evaluated and (c) pore size distribution after application of the QSDFT method to the nitrogen adsorption data (slit-shaped pore model).

3. Results and discussion

3.1. Evaluation of the porous structure

The porous structure of the synthesized carbon materials has been evaluated using gas adsorption measurements. N_2 adsorption at cryogenic temperatures (−196 °C) has been applied to evaluate the micro-/mesoporous network, while CO_2 adsorption at 0 °C has been used to evaluate the narrow microporous structure. Fig 1 compares the adsorption of these two probes, N_2 and CO_2, up to atmospheric pressure, while textural characteristics are reported in Table 2.

Condensed cysteine (not shown) exhibits a flat isotherm due to the absence of accessible porosity after the thermal treatment at 700 °C ($S_{BET} = 2$ m²/g). Contrary to previous results obtained with

guanine condensates (200 m²/g were reached at 700 °C) [26], our results reflects the necessity to incorporate an additional activation step to develop porosity in the obtained cysteine-based solid condensates. The results described in Fig 1 show that, for a given activation temperature (e.g., 800 °C), the porous structure of the synthesized samples scales-up with the extend of the activation treatment, i.e. activation time from 1 h to 6 h. Sample activated for 1 h at 800 °C, i.e. CAC1800, exhibits a poorly developed porous structure, with a BET surface area ca. 140 m²/g (see Table 2). The presence of a scarcely developed porous structure can be clearly appreciated in the N_2 adsorption isotherm (Type I according to the IUPAC classification), with a narrow knee at low relative pressures associated with a purely microporous material and a limited adsorption capacity. An extension in the activation process to 3 h and 6 h at 800 °C gives rise to a significant development of the poros-

Table 2
Textural parameters deduced from the nitrogen and CO_2 adsorption measurements.

Sample	S_{BET} (m²/g)	V_0 (cm³/g)	V_{meso} (cm³/g)	V_{total} (cm³/g)	V_n CO_2 (cm³/g)
CAC1800	141	0.06	0.01	0.07	0.18
CAC3800	600	0.25	0.01	0.26	0.24
CAC6800	1013	0.42	0.01	0.43	0.26
CAC1900	378	0.17	0.01	0.18	0.11

ity with a BET surface area of 600 m²/g and 1013 m²/g, respectively. Interestingly, the N_2 adsorption isotherms confirm that the activation treatment with CO_2 provides purely microporous samples, independently of the activation degree. The exclusive presence of microporosity is also reflected in Table 2 ($V_{meso} \sim 0$ cm³/g for all samples) and in the pore size distribution estimated after application of the QSDFT method (Fig 1c). Despite these large differences in the nitrogen adsorption performance for the three samples synthesized at 800 °C, their CO_2 uptake (Fig 1b) at 0 °C and 1 bar is rather similar. This observation anticipates the presence of diffusional restrictions for N_2 to access the inner porous structure in samples with a low activation degree (e.g., CAC1800). The restricted accessibility for nitrogen at −196 °C is confirmed after comparing the micropore volume (V_0) and the narrow micropore volume (V_n) deduced after application of the Dubinin-Radushkevich equation to the N_2 and CO_2 isotherms, respectively. For this specific sample $V_n >> V_0$, thus confirming the presence of diffusional restrictions for nitrogen to access the inner porous structure at cryogenic temperatures [28]. The presence of narrow micropores is also reflected in the more concave shape of the CO_2 isotherm at 0 °C. In the specific case of sample CAC3800, $V_n \sim V_0$, thus reflecting the presence of a narrow micropore size distribution. Only sample CAC6800 possess wider micropores ($V_0 >> V_n$), although without mesoporosity. This sample exhibits a BET surface area as high as 1013 m²/g. At this point it is important to highlight that although the CO_2 adsorption isotherms could be slightly affected by surface functional groups, their presence does not allow to explain the observed differences between N_2 and CO_2. Overall, these results show that L-cysteine is an excellent platform to synthesize purely microporous activated carbons with, *a priori*, molecular sieving properties.

An additional carbon sample was prepared through an activation treatment at 900 °C for 1 h. Sample CAC1900 exhibits a moderate BET surface area (ca. 378 m²/g). Compared to sample CAC1800, the increase in the activation temperature allows to widen the porosity, thus avoiding, *a priori*, the aforementioned restrictions for nitrogen to access the inner porous structure. However, the sample activated at 900 °C for 1 h exhibits a surprisingly small volume of narrow micropores (although BET is much higher), thus reflecting some potential limitations for CO_2 to access the narrow porosity, as will be discussed later on.

3.2. Evaluation of the morphology of the synthesized carbons

Once the porous structure is well-stablished, the next open question concerns the morphology of the synthesized carbon particles. To gain insights about the morphology, we have performed field emission scanning electron microscopy (FE-SEM) in the synthesized samples. Fig 2 shows some representative pictures of samples CACx800 ($x = 1$–6). As it can be appreciated in the microscopy images, the morphology of the synthesized activated carbons is quite unique and complex. Samples with a low activation degree (e.g., CAC1800) show a quite regular morphology with a perfectly smooth surface (Fig 2a). However, after a higher activation degree (3 h and 6 h at 800 °C) the morphology of the samples

becomes irregular and new structures can be appreciated. FE-SEM images allow to discern sections with the formation of needles (Fig 2b), sections with holes in the macroporous range (Figs 2b-d), and sections with globular-based structures (Fig 2e). Similar morphologies have been reported in the literature by Cosmidis and coworkers after organomineralization of dissolved sulfide and dissolved organics (sugars and amino acids) in the presence of oxygen [29]. According to these authors, the needles and globular structures correspond to S(0) phases, preferentially β-, α- or γ-S_8, associated with the organics and obtained after a self-assembly mechanism. Apparently, the dissolved organic molecules (e.g., amino acids) are able to polymerize into solid, macromolecular, polymeric organics stabilizing S(0) particles in their core. Considering that cysteine is an amino acid containing sulphur functionalities, one can speculate that the decomposition of these functional groups during the activation treatment with CO_2 at high temperature can help the remaining organics to polymerize into similar needle-shape and globular structures containing most probably S_8 in close association with the organic phase.

3.3. Evaluation of the surface chemistry

As described in the introduction, L-cysteine is a potential platform to synthesize multifunctional activated carbons. The nature of the surface functionalities has been evaluated using X-ray photoelectron spectroscopy. XPS is a very useful tool to obtain information about the chemical and electronic characteristics of the activated carbon surface. Table 3 shows the oxygen, nitrogen and sulphur content in the different samples evaluated determined from the XPS spectra. Due to the heterogeneity of the synthesized carbon materials, the chemical analysis has been performed in three different regions of the sample. As expected, the activated carbons produced from L-cysteine contain carbon, oxygen, nitrogen and sulphur in their composition. The original cysteine (not shown) contains 21 at. % of oxygen, 8 at. % of nitrogen and 11 at. % of sulphur. After the condensation/carbonization and activation treatment all samples preserve the three functionalities although with a different percentage. In general, the thermal treatments applied in the synthesis of the carbon materials (e.g., CAC1800) give rise to a significant decrease in the concentration of all the aforementioned functional groups. Overall, sulphur is more unstable with a decrease of 66% compared to the original amino acid, followed by nitrogen (48% decrease) and oxygen functionalities (49% decrease). In any case, the results described in Table 3 confirm that activated carbons prepared from L-cysteine preserve a rich surface chemistry combining the three groups, although with a certain heterogeneity (see differences in the three points analysed). A subsequent increase in the activation time to 3 h, sample CAC3800, modifies significantly the percentage of these groups, i.e. there is a significant decrease in the content of nitrogen and sulphur, while the amount of oxygen is highly increased. Last but not least, the sample prepared at 800 °C during 6 h exhibits a similar trend. There is an increase in the amount of oxygen surface groups (up to 25 at.%), together with a decrease in the percentage of nitrogen and sulphur groups. A comparison of samples CAC1×00 shows that the surface
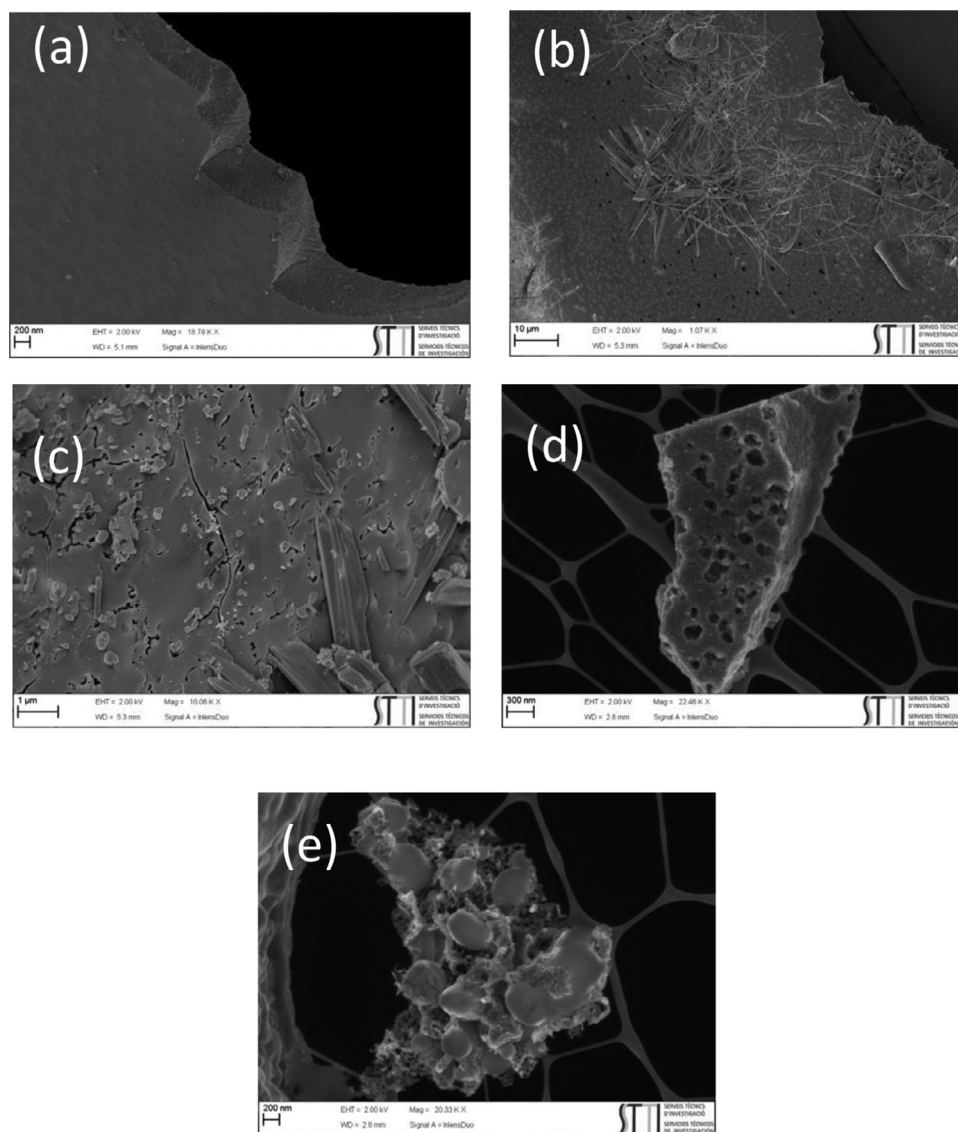
Fig 2. FE-SEM images of samples (a) CAC1800, (b) CAC3800 and (c-e) CAC6800.

Table 3
Oxygen, nitrogen and sulphur content (at.%) for the different samples evaluated obtained from the XPS spectra. Analysis have been performed in three different positions of the sample to identify the presence of heterogeneities. Average values are included in hyphens.

Sample	C (at.%)	O (at.%)	N (at.%)	S (at.%)
CAC1800	82.7/83.4/77.9 – 81.3 –	10.0/9.0/13.2 – 10.7 –	4.1/4.4/4.1 – 4.2 –	3.2/3.2/4.8 – 3.7 –
CAC3800	78.0/69.6/72.9 – 73.5 –	16.1/25.9/21.6 – 21.2 –	3.9/2.6/3.5 – 3.3 –	2.0/1.9/2.0 – 2.0 –
CAC6800	71.5/73.2/67.1 – 70.4 –	24.2/22.5/28.7 – 25.1 –	2.6/2.5/2.4 – 2.5 –	1.7/1.7/1.7 – 1.7 –
CAC1900	77.3/76.3/75.8 – 76.5 –	17.5/18.9/18.6 – 18.4 –	3.3/2.5/3.2 – 3.0 –	1.9/2.2/2.4 – 2.2 –

chemistry is slightly different at 800 °C and 900 °C, i.e. the more unstable nitrogen and sulphur groups decrease significantly, while a significant increase in the amount of oxygen functional groups is observed.

A careful evaluation of the XPS core levels for C1s, O1s, N1s and S2p is reported in Fig 3. At this point it is important to highlight that due to the similarity in the XPS spectra of the synthesized samples, only the spectra for sample CAC6800 is re-

ported. The N1s signal shows two well-defined contributions at 398.5 eV and 400.8 eV. These contributions are typically observed in N-doped activated carbons and correspond to pyridinic-N and pyrrolic/pyridonic-N functional groups, respectively, thus confirming the successful incorporation of the nitrogen functionalities in the graphene microdomains [30,31]. The ratio of pyridinic-N to pyrrolic/pyridonic-N groups is around 0.73–0.87 for the three samples evaluated. The XPS spectra of sulphur is characterized in all
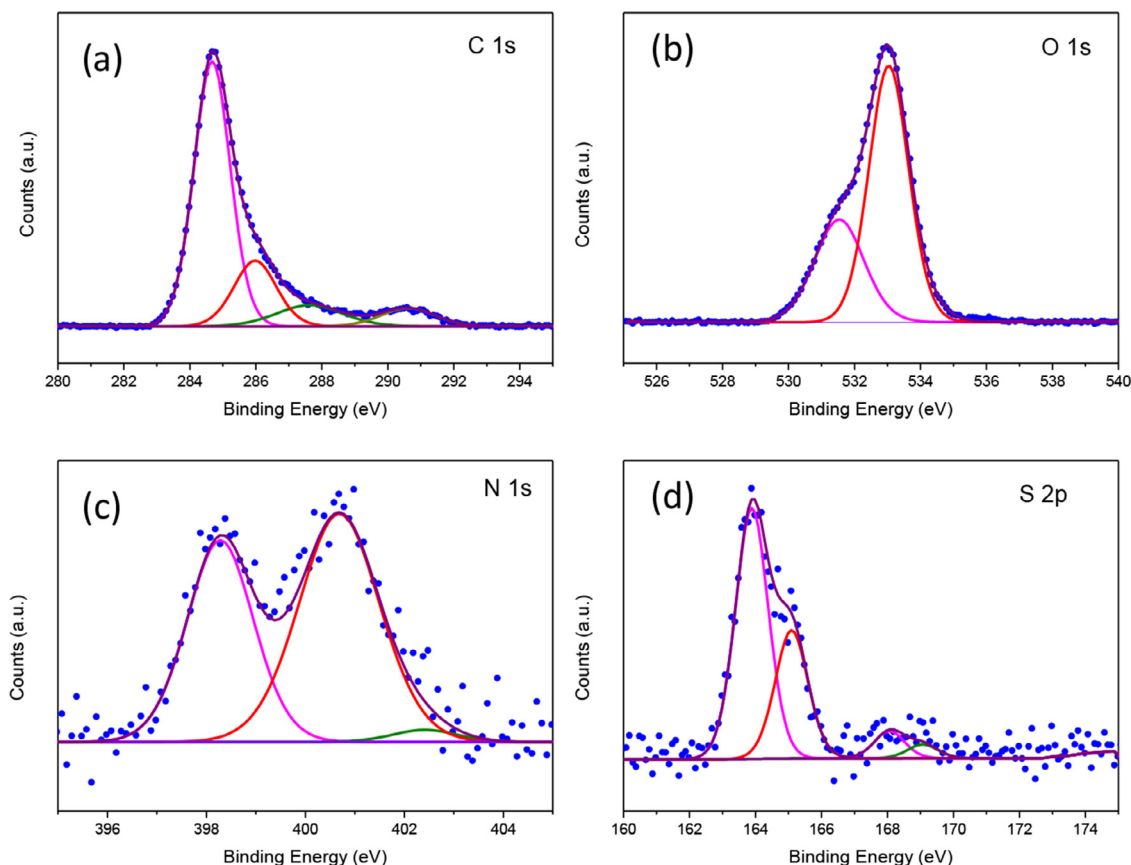
Fig 3. XPS spectra in the (a) C1s, (b) O1s, (c) N1s and (d) S2p region for sample CAC6800.

samples by a doublet due to S $2p_{3/2}$ and S $2p_{1/2}$ with an energy of 163.9–164.0 eV and 165.2–165.4 eV, respectively. The intensity ratio between the two signals is ca. 2:1. The binding energy observed for the S $2p_{3/2}$ contribution is rather similar to that described in the literature for elemental sulphur (S_8) at 164.0 eV. This observation would be in agreement with the needles and globular structures observed above in the FE-SEM images. However, the broad nature of the peak at 163.9 eV does not exclude the additional presence of sulphur incorporated in the graphene planes as C−S species at a binding energy of 163.8 eV. In all cases, a minor contribution (27%) appears at 168.6 eV attributed to sulphate species (C-SO$_x$-C) in the carbon structure [32]. The XPS spectra of O1s has been deconvoluted in two main contributions at 531.3 eV and 532.8 eV [33]. Previous studies described in the literature have assigned these groups to carbonyl oxygen of quinones (C=O at 531.0–531.9 eV), and carbonyl oxygen atoms in esters, anhydrides and oxygen atoms in hydroxyl groups (C−O at 532.3–532.8 eV) [30,33]. Last but not least, the XPS spectra of the C1s gives rise to a broad contribution in the 283–291 eV range, for all samples. The C1s signal can be deconvoluted in four contributions, the main one at 284.7 eV and three decreasing shoulders at 285.8 eV, 287.2 eV, and 289.4 eV. According to the literature, the main contribution corresponds to C−C and C=C bonds, while the shoulders must be attributed to C−N or C−S at 285.8 eV, C=O at 287.2 eV and O−C=O at 289.4 eV.

In summary, XPS data confirm the presence of a rich surface chemistry in the synthesized samples, with the concomitant presence of oxygen, nitrogen and sulfur functional groups. These groups are incorporated in the carbon network in different morphologies (e.g., carbonyl, carboxyl, etc.), their nature being rather independent of the preparation conditions. Amongst these groups sulphur is the most unstable followed by nitrogen whereas the oxygen content increases with the activation treatment applied.

3.4. Adsorption of target molecules

As described in the introduction, L-cysteine is an amino acid that contains oxygen, nitrogen and sulphur functional groups in its structure. The presence of three different functionalities in a single molecule makes it an attractive platform to produce carbon materials with a rich multicomponent surface chemistry, avoiding inconvenient and expensive post-synthesis treatments. It is well-known in the literature that the presence of oxygen functionalities in carbon materials modifies the adsorption of polar molecules, e.g., carbon-water interactions, through a cluster-mediated pore-filling mechanism [10–13]. The adsorption mechanism is based on the formation of hydrogen-bonds between the adsorbed water molecules and the oxygen surface groups, acting a primary adsorption sites. While non-functionalized activated carbons are mainly hydrophobic in nature (water adsorption isotherms are of Type V), the presence of oxygen functionalities changes the isotherms gradually to a Type IV, while the inflection point defining the micropore filling is shifted to lower relative pressures. Although it is far less explored, the incorporation of nitrogen functional groups to the carbon surface increases the affinity for water molecules at a low relative humidity [34–37]. In the specific case of sulphur, there are no studies in the literature dealing with the effect of these functionalities in the water adsorption performance. However, Seredych et al. reported an improved polarity for carbon materials modified with H_2S with enhanced adsorption potential for benzothiophenic molecules [38]. With these premises, it is obvious that activated carbons rich in oxygen, nitrogen and sulphur must have *a priori* enhanced adsorbent-adsorbate interactions for polar molecules, such as water. H_2O adsorption isotherms described in Fig 4 confirm this assumption with Type VI isotherms for all cysteine-based samples. Three distinct regions can be clearly ap-
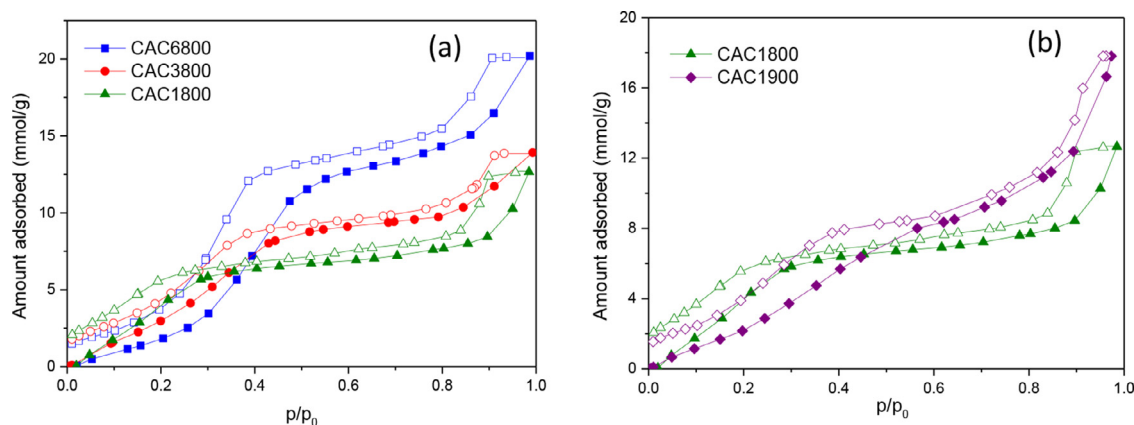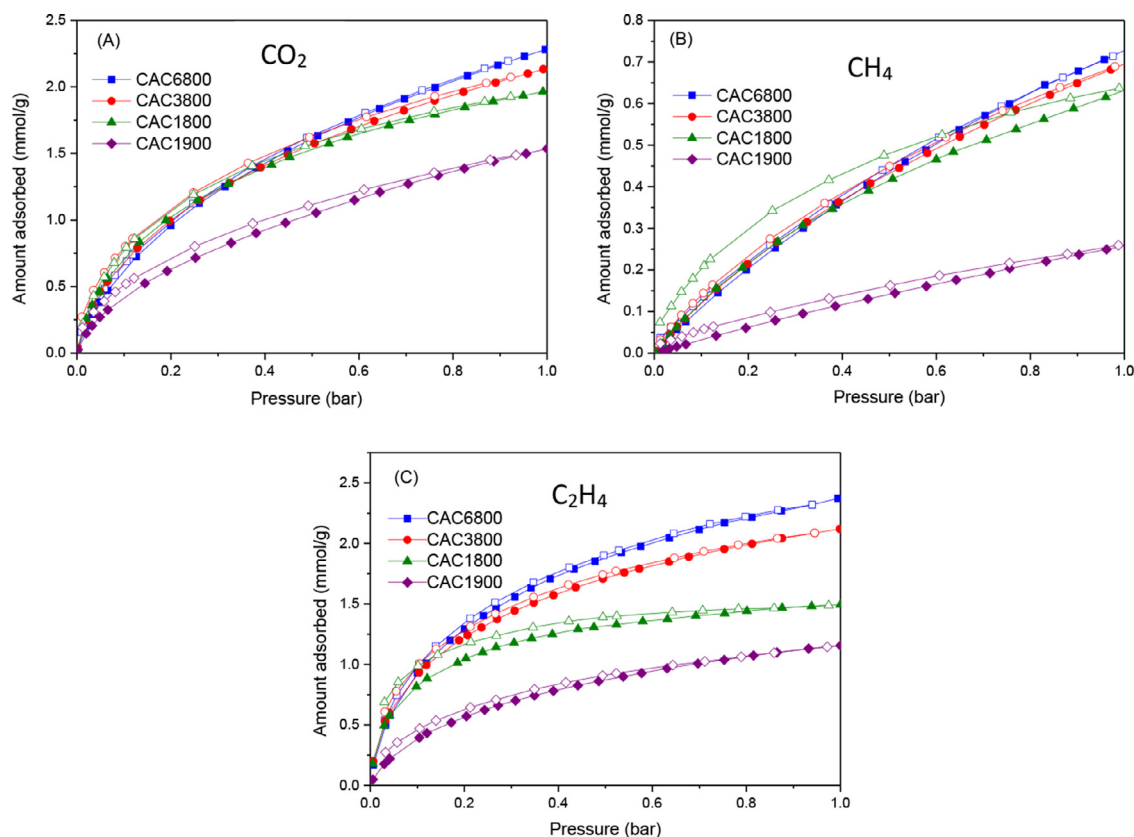
Fig 4. Water adsorption/desorption isotherms at 25 °C for the different cysteine-based samples: (a) samples CACx800 and (b) samples CAC1×00.

preciated. At low relative pressures, water isotherms exhibit a linear performance up to $p/p_0 \approx 0.3$ (see Fig 4a). Interestingly, the initial linear section is steeper for samples with a lower activation degree, with a significant shift in the onset to lower relative pressures. This result clearly reflects the crucial role of the surface chemistry in water adsorption at low relative pressures. In the sample with the lowest activation degree, i.e. CAC1800, this linear region reaches a plateau above $p/p_0 \approx 0.3$, thus reflecting the completion in the filling of the narrow micropores. Narrow micropores with an enhanced adsorption potential are easily saturated with water at low relative pressures, in agreement with theoretical predictions [11]. Samples with a higher activation degree (CAC3800 & CAC6800) exhibit an additional inflection point above $p/p_0 \approx 0.3$ attributed to water condensation in wider micropores (cooperative adsorption mechanism in surface water clusters) until a plateau is reached. As expected, the total amount adsorbed at the plateau scales-up with the activation degree, i.e. more micropores are available to adsorb water molecules. However, differences in the uptake at the plateau ($p/p_0 \approx 0.6$) amongst samples are smaller than those observed above for N_2 adsorption at cryogenic temperatures (sample CAC1800 does not differ significantly from sample CAC3800). This is another evidence about the presence of kinetic restrictions for N_2, with a larger kinetic diameter (0.36 nm for N_2 vs 0.28 nm for H_2O), to access some of the inner cavities in sample CAC1800. Above $p/p_0 \approx 0.8$ all samples exhibits a final adsorption step most probably associated with the condensation in the interparticle space. In all cases, the desorption branch exhibits two hysteresis loops, one at mid-relative pressures and one at low-relative pressures. This observation reflects the metastability of water adsorption in activated carbon materials. A comparison of samples activated for 1 h using two different temperatures, 800 °C and 900 °C, confirms these findings. The presence of wider pores in sample CAC1900 and a poorer surface chemistry gives rise to a shift in the water affinity to higher pressures and less market plateau. However, contrary to nitrogen at cryogenic temperatures, where kinetic restrictions are evident, water molecules with a kinetic diameter around 0.28 nm are able to access the inner porosity in sample CAC1800 in a similar fashion to sample CAC1900. Even the differences observed in Fig 1 for CO_2 adsorption at a higher adsorption temperature (0 °C), CAC1800>>CAC1900, are washed out when using water as a probe molecule. This observation could be an indication of the presence of kinetic restrictions in sample CAC1900 due to the presence of extremely narrow micropores not accessible to CO_2 at 0 °C.

Once the porous structure and the nature of the surface functional groups has been carefully analysed, the open question at this point is how these activated carbons prepared from L-cysteine per-

form in the adsorption of two important target molecules, CH_4 and CO_2 adsorption. Previous studies described in the literature have shown that the porous structure of the carbon materials, i.e. the presence of narrow pores able to reach a high packing density, is the main factor defining the adsorption performance for these two probes [39–41]. In the specific case of CO_2, narrow micropores (below 0.6 nm) exhibit an optimum performance for gas adsorption at atmospheric pressure whereas larger pores (below 2–3 nm) govern the adsorption performance at high pressures [41]. A similar scenario is predicted for methane adsorption in activated carbon materials. Grand Canonical Monte-Carlo simulations anticipate an optimum performance in pores around 0.8 nm for methane adsorption at atmospheric pressure, i.e. cavities able to accommodate two adsorbed layers of methane [42,43]. Concerning the role of the surface functionalities in the adsorption of these two molecules the situation is more controversial. The most widely evaluated molecule has been CO_2. Previous studies described in the literature have shown that, in principle, all surface functionalities exhibit a certain effect in CO_2 adsorption, although relatively small compared to the effect of the porous network. These studies include the evaluation of oxygen [25], nitrogen [17,18,25,44], sulphur [21,45] and phosphorus groups [25]. In general, it is widely accepted that the presence of nitrogen functionalities, preferentially N basic sites (e.g., pyridonic and pyrrolic groups), enhance the adsorption capacity of carbon materials towards CO_2 [17,18,25]. A similar situation takes place after incorporation of sulphur functional groups [21,45]. The presence of sulphur in the graphene layers modifies the surface charge (it can bring a slightly positive charge to neighbouring carbon atoms) and provides some basicity, thus promoting the CO_2-surface interactions. Overall, the results published in the literature anticipate an important role of the porous structure in the adsorption performance for CO_2, while the effect of the surface chemistry, although appreciable, it is less important and differs depending of the amount and nature of the surface functional groups. Contrary to CO_2, the effect of the surface chemistry in the adsorption of methane has not been documented in the literature, thus anticipating a residual role of the surface chemistry, if any, in the adsorption of methane.

Fig 5 shows the adsorption/desorption isotherms for (a) CO_2, (b) CH_4 and (c) C_2H_4 at 25 °C and up to 1 bar for the different carbon materials evaluated. As it can be appreciated, the amount of CO_2 adsorbed at 25 °C is smaller than that reported before at 0 °C (see Fig 1a), except for sample CAC1900 with a slight increase (8%). The decrease in the amount adsorbed is supported by thermodynamic considerations, while in the case of sample CAC1900 the increase uptake at 25 °C confirms the presence of narrow constrictions not accessible for CO_2 at 0 °C. As expected, the knee of

Fig 5. Adsorption/desorption isotherms for (a) CO_2, (b) CH_4 and (c) C_2H_4 at 25 °C in the different carbon materials evaluated.

the isotherm widens with the activation degree, with a final uptake slightly larger for sample CAC6800 (up to 2.3 mmol/g). These results confirm the widening of the porosity with the activation time, together with the presence of kinetic restrictions, even at 25 °C, for sample CAC1900 (also reflected by the presence of a significant hysteresis loop). The uptake obtained with cysteine-based samples (ca. 2.0–2.3 mmol/g) constitutes a significant improvement compared to guanine condensates prepared at 700 °C without activation step [26]. Adsorption of methane under similar pressure and temperature conditions gives rise to a similar performance. Samples CACx800 exhibit a type I shape isotherm due to the presence of narrow micropores able to accommodate methane. However, the larger kinetic diameter of methane vs. CO_2 (0.39 nm vs. 0.33 nm) is reflected by a significant hysteresis loop in sample CAC1800, thus suggesting some accessibility issues. A similar scenario takes place for sample CAC1900 with a rather linear profile. Apparently, activation for 1 h gives rise to cavities with narrow constrictions similar in size to the methane molecule, thus inferring severe restrictions to methane to access the inner porous structure (molecular sieving properties, mainly in CAC1900 sample).

The differences in the porous structure amongst samples are also reflected in the gas adsorption isotherms for larger hydrocarbons (e.g., C_2H_4). Overall the total adsorption uptake is much larger for C_2H_4 compared to CH_4, i.e. adsorption of larger hydrocarbons in supercritical conditions is enhanced due to the stronger adsorption potential in the porous network. Samples CAC3800 and CAC6800 with a widely developed porous structure are able to adsorb up to 2.1 and 2.4 mmol/g, respectively. However, the amount adsorbed drastically decreases for sample CAC1800 (ca. 1.5 mmol/g) due to the presence of inaccessible narrow micropores. A similar situation takes place for sample CAC1900, with a poor adsorption performance (total uptake close to 1.2 mmol/g). These observations

anticipate that samples CAC1800 and CAC1900 are carbon molecular sieves with narrow pore size windows.

In order to better understand the adsorption performance of the cysteine-based carbons, the total uptake at 1 bar for CO_2, CH_4 and C_2H_4 has been plotted versus the narrow micropore volume (V_n), obtained from the CO_2 adsorption data at 0 °C after application of the Dubinin-Radushkevich equation. Fig 6A clearly shows that the performance for each of these probes differs depending on its chemical characteristics. Overall carbon dioxide adsorption exhibits a progressive increase, mainly linear, with an increase in the narrow micropore volume. A similar situation takes place for methane. However, there are two important differences between these two probes: i) the slope is much larger for CO_2, i.e. the development of wider micropores has a higher beneficial effect for subcritical CO_2 adsorption versus supercritical CH_4 adsorption at 25 °C and ii) the amount adsorbed at $V_n \to 0$ is much higher for CO_2 (ca. 1.3 mmol/g) versus CH_4 (ca. 0.4 mmol/g). This observation could be an indication of the role of the surface chemistry for both probes, i.e. the presence of a rich surface chemistry containing O, N and S will have a beneficial effect in the amount of CO_2 adsorbed while the effect of these groups in the adsorption of CH_4 will be rather small. Although the role of the porosity is similar for larger hydrocarbons (uptake increases with V_n), the slope is much larger for C_2H_4, thus anticipating the important role of wide micropores for an optimum adsorption of ethylene. Fig 6 anticipates that sample CAC1900 (dashed points) does not follow any tendency most probably due to the restricted accessibility for the three probes at 25 °C, as described above. The variations in the adsorption performance with the activation degree are also reflected in the selectivity ratio, i.e. $S_{CO2/CH4}$ and $S_{C2H4/CH4}$. The selectivity ratio is very similar for CACx800 samples with a value around 3.2 for $S_{CO2/CH4}$. In the case of C_2H_4/CH_4, the selectivity ratio increases with the activation
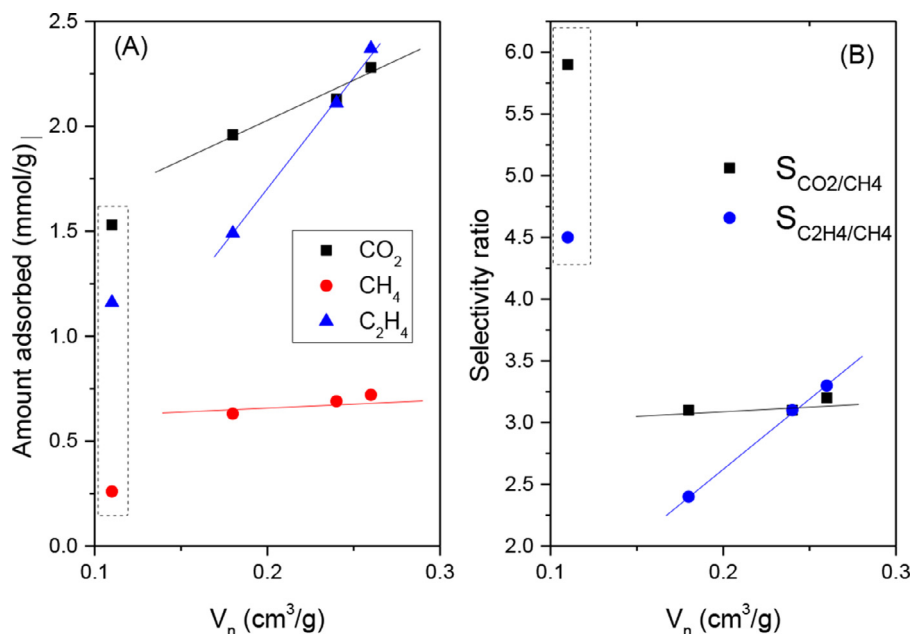
Fig 6. Correlation between (A) the amount adsorbed for the three probe molecules evaluated and (B) selectivity ratio $S_{CO2/CH4}$ and $S_{C2H4/CH4}$ as a function of the narrow micropore volume (V_n).
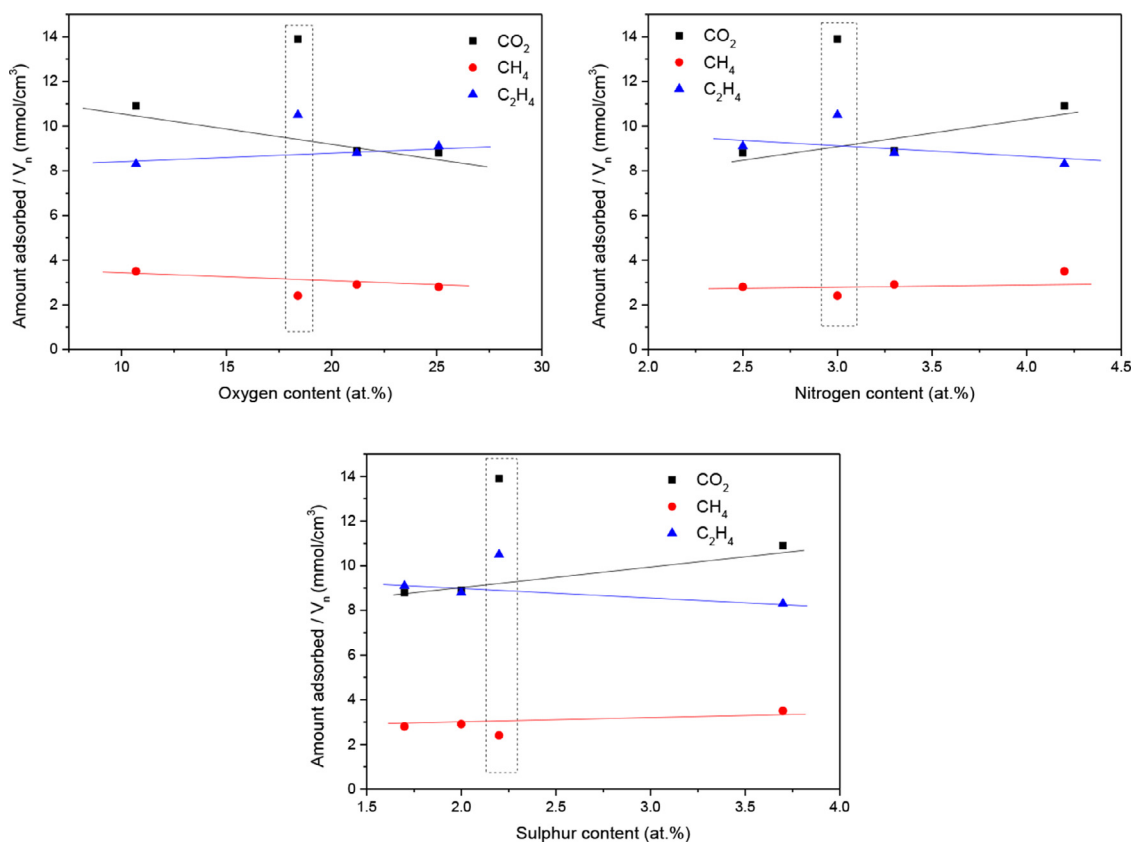
Fig 7. Correlation between the amount of adsorbed for the three probes at 1 bar and 25 °C, normalized with the narrow micropore volume, and the atomic% of functional groups obtained from the XPS data.

degree (up to 3.3) due to the dominant role of wide micropores in the adsorption of larger hydrocarbons. Interestingly, these values drastically increase for a carbon molecular sieve with narrow constrictions, such as sample CAC1900, with values up to $S_{CO2/CH4} = 6$ and $S_{C2H4/CH4} = 4.5$. A CO$_2$/CH$_4$ selectivity value at equilibrium of 6, with a total uptake for CO$_2$ of 1.5 mmol/g is a very good value compared to other carbon materials reported in the literature [46].

Last but not least, the amount of CO$_2$, CH$_4$ and C$_2$H$_4$ adsorbed at 1 bar and 25 °C has been compared with the evolution of the surface functional groups, obtained from the XPS data. In order to

minimize the effect of the porous structure (both surface chemistry and porous structure varies with the activation degree) and emphasize the effect of the surface chemistry, the amount adsorbed for the three probes has been normalized using the narrow micropore volume (V_n). As it can be observed in Fig 7, the role of the surface chemistry in the adsorption of the three probes evaluated (mmol/cm^3) is quite small. In all three cases sample CAC1900 (dashed box) deviates from the "normal" behaviour due to the presence of kinetic restrictions. Excluding this sample from the discussion, some hints can be appreciated about the role of the surface functional groups. In general, the results described in Fig 7 show that neither oxygen, nitrogen nor sulphur functional groups have a significant effect in the amount of methane adsorbed. This observation will be in agreement with the "inert" character of the methane molecule (i.e., spherical non-polar molecule). A similar scenario takes place for a larger hydrocarbon such as C_2H_4. In general, the effect of the functional groups is small, although a certain detrimental effect can be appreciated for nitrogen and sulphur functionalities, while oxygen slightly improves the amount adsorbed. The situation is different for a more "reactive" molecule such as CO_2 with a soft acidic character. In this case, nitrogen and sulphur groups have a clear promoting effect, in close agreement with previous results in the literature [17,21,25]. This observation can be explained due to the basic character of the N (pyridinic-N and pyrrolic/pyridonic-N) and sulphur groups incorporated in the carbon network and the promoting acid-base interactions. Contrariwise, oxygen surface groups have a negative effect in the uptake of CO_2 due to their acidic nature [25]. However, care must to be taken with these assumptions due to the large heterogeneity of these carbon materials and the uncertainty in the amount of oxygen, nitrogen and sulphur groups.

4. Conclusions

In summary, we have demonstrated that amino acids such as L-cysteine are potential platforms to synthesize activated carbon materials combining a highly developed porous structure and rich surface chemistry. Through a physical activation with CO_2, carbon materials can be designed from carbon molecular sieves (for low activated samples) to samples combining narrow and wide micropores. XPS analysis confirm that the synthesized carbons exhibit a rich surface chemistry containing oxygen, nitrogen and sulphur functional groups. The presence of these functionalities modifies the physicochemical characteristics of the carbon materials, thus promoting the adsorbate-adsorbent interactions with polar molecules (e.g., H_2O). Although the effect of the surface chemistry is less clear for non-polar probes (e.g., CH_4, C_2H_4 and CO_2), a careful analysis anticipates that nitrogen and sulphur groups have a slightly positive effect for CO_2 adsorption, while oxygen functionalities become detrimental. As expected, the effect of the surface chemistry is rather insignificant for the evaluated hydrocarbons, mainly for CH_4. The synthesized carbons exhibit a proper CO_2 uptake (up to 3 mmol/g at 0 °C). Furthermore, samples with a low activation degree exhibit molecular sieving properties with very promising CO_2/CH_4 (up to 4.5) and C_2H_4/CH_4 (up to 6) selectivity.

Declaration of Competing Interest

The authors declare that they have no known competing financial interests or personal relationships that could have appeared to influence the work reported in this paper.

CRediT authorship contribution statement

S. Reljic: Conceptualization, Investigation, Formal analysis. **C. Cuadrado-Collados:** Conceptualization, Methodology. **E. Oliveira Jardim:** Methodology, Formal analysis. **J. Farrando-Perez:** Investigation. **M. Martinez-Escandell:** Writing – review & editing. **J. Silvestre-Albero:** Project administration, Supervision, Funding acquisition.

References

[1] H. Marsh, F. Rodríguez-Reinoso, Activated Carbon (2006).
[2] J. Hao, X. Li, X. Song, Z. Guo, Recent progress and perspectives on dual-ion batteries, EnergyChem 1 (2019) 100004.
[3] Y. Lei, X. Liang, L. Yang, P. Jiang, Z. Lei, S. Wu, J. Feng, Novel hierarchical porous carbon prepared by a one-step template route for electrical double layer capacitors and Li-Se battery devices, J. Mater. Chem. A 8 (2020) 4376–4385.
[4] N.A. Travlou, M. Seredych, E. Rodríguez-Castellón, T.J. Bandosz, Activated carbon-based sensors: effects of surface features on the sensing mechanism, J. Mater. Chem. A 3 (2015) 3821–3831.
[5] M. Sevilla, R. Mokaya, Energy storage applications of activated carbons: supercapacitors and hydrogen storage, Energy & Environm. Sci. 7 (2014) 1250–1280.
[6] S. Sircar, T.C. Golden, M.B. Rao, Activated carbon for gas separation and storage, Carbon 34 (1996) 1–12.
[7] T. Bandosz, Surface chemistry of carbon materials, in: P. Serp, J.L Figueiredo (Eds.), Carbon Materials For Catalysis, Wiley, 2009, pp. 45–92. Eds..
[8] D. Saha, M.J. Kienbaum, Role of oxygen, nitrogen and sulfur functionalities on the surface of nanoporous carbons in CO_2 adsorption: a critical review, Microp. Mesop. Mater. 287 (2019) 29–55.
[9] V.L. Snoeyink, W.J. Weber, The surface chemistry of active carbon; a discussion of structure and surface functional groups, Environ. Sci. Technol. 1 (1967) 228–234.
[10] E.A. Müller, F.R. Hung, K.E. Gubbins, Adsorption of water vapor-methane mixtures on activated carbons, Langmuir 16 (2000) 5418–5424.
[11] A.M. Slasli, M. Jorge, F. Stoeckli, N.A. Seaton, Water adsorption by activated carbons in relation to their microporous structure, Carbon 41 (2003) 479–486.
[12] A. Tóth, K. László, Water Adsorption By carbons. Hydrophobicity and hydrophilicity, in Novel Carbon Adsorbents (J.M.D. Tascón, Ed.), 2012, Elsevier, pp. 147–171.
[13] A.J. Fletcher, Y. Uygur, K.M. Thomas, Role of surface functional groups in the adsorption kinetics of water vapor on microporous activated carbons, J. Phys. Chem. C 111 (2007) 8349–8359.
[14] S.E. Kim, S.K. Jeong, K.T. Park, K.-Y. Lee, H.J. Kim, Effect of oxygen-containing functional groups in metal-free carbon catalysts on the decomposition of methane, Catal. Commun. 148 (2021) 106167.
[15] T.S. Blankenship, N. Balahmar, R. Moyaka, Oxygen-rich microporous carbons with exceptional hydrogen storage capacity, Nature Commun 8 (2017) 1545.
[16] C. Pevida, M.G. Plaza, B. Arias, J. Fermoso, F. Rubiera, J.J. Pis, Surface modification of activted carbons for CO_2 capture, Appl. Surf. Sci. 254 (2008) 7165–7172.
[17] M. Sevilla, P. Valle-Vigon, A.B. Fuertes, N-doped polypyrrole-based porous carbons for CO_2 capture, Adv. Funct. Mater. 21 (2011) 2781–2787.
[18] G.-P. Hao, W.-C. Li, D. Qian, A.-H. Lu, Rapid synthesis of nitrogen-doped porous carbon monolith for CO_2 capture, Adv. Mater. 22 (2010) 853–857.
[19] T. Cordero-Lanzac, J.M. Rosas, F.J. Garcia-Mateos, J.J. Ternero-Hidalgo, J. Palomo, J. Rodríguez-Mirasol, T. Cordero, Role of different nitrogen functionalities on the electrochemical performance of activated carbons, Carbon 126 (2018) 65–76.
[20] Q. Lv, W. Si, J. He, L. Sun, C. Zhang, N. Wang, Z. Yang, X. Li, X. Wang, W. Deng, Y. Long, C. Huang, Y. Li, Selectively nitrogen-doped carbon materials as superior metal-free catalysts for oxygen reduction, Nature Commun 9 (2018) 3376.
[21] M. Seredych, J. Jagiello, T.J. Bandosz, Complexity of CO_2 adsorption on nanoporous sulfur-doped carbons - Is surface chemistry an important factor? Carbon 74 (2014) 207–217.
[22] A.D. Roberts, X. Li, H. Zhang, Hierarchically porous sulfur-containing activated carbon monoliths via ice-templating and one-step pyrolysis, Carbon 95 (2015) 268–278.
[23] X. Qi, W. Chen, J. Zhang, Sulphur-doped activated carbon as a metal-free catalyst for acetylene hydrochlorination, RSC Adv 10 (2020) 34612–34620.
[24] N. Asasian, T. Kaghazchi, Sulfurized activated carbons and their mercury adsorption/desorption behavior in aqueous phase, Int. J. Environ. Sci. Technol. 12 (2015) 2511–2522.
[25] A. Sanchez-Sanchez, F. Suarez-Garcia, A. Martinez-Alonso, J.M.D. Tascon, Influence of porous texture and surface chemistry on the CO2 adsorption capacity of porous carbons: acidic and basic site interactions, ACS Appl. Mater. Interfaces 6 (2014) 21237–21247.
[26] J. Kossmann, D. Piankova, N.V. Tarakina, J. Heske, T.D. Kühne, J. Schmidt, M. Antonietti, N. López-Salas, Guanine condensates as covalent materials and the concept of cryptopores, Carbon 172 (2021) 497–505.

[27] N. Izzah Ismail, Y.Z. Has-Yun Hashim, P. Jamal, R. Othman, H. Mohd Salleh, Production of cysteine: Approaches, Challenges and Potential Solution, Inter. J. Biotechn. Wellness Ind. 3 (2014) 95–101.

[28] R.V.R.A. Rios, J. Silvestre-Albero, A. Sepúlveda-Escribano, M. Molina-Sabio, F Rodríguez-Reinoso, Kinetic restrictions in the characterization of narrow microporosity in carbon materials, J. Phys. Chem. C 111 (2007) 3803–3805.

[29] J. Cosmidis, C.W. Nims, D. Diercks, A.S. Templeton, Formation and stabilization of elemental sulfur through organomineralization, Geochim. Cosmochim. Acta 247 (2019) 59–82.

[30] M. Ayiania, M. Smith, A.J.R. Hensley, L. Scudiero, J.-S. McEwen, M. García-Perez, Deconvoluting the XPS spectra for nitrogen-doped chars: An analysis from first principles, Carbon 162 (2020) 528–544.

[31] P. Wu, Y. Qian, P. Du, H. Zhang, C. Cai, Facile synthesis of nitrogen-doped graphene for measuring the releasing process of hydrogen peroxide from living cells, J. Mater. Chem. 22 (2012) 6402–6412.

[32] Z. Wang, Y. Dong, H. Li, Z. Zhao, H.B. Wu, C. Hao, S. Liu, J. Qiu, X.W.D. Lou, Enhancing lithium-sulphur battery performance by strongly binding the discharge products on amino-acid functionalized reduced graphene oxide, Nature Commun 5 (2014) 5002.

[33] J.-H. Zhou, Z.-J. Sui, J. Zhu, P. Li, D. Chen, Y.-C. Dai, W.-K. Yuan, Characterization of surface oxygen complexes on carbon nanofibers by TPD, XPS and FT-IR, Carbon 45 (2007) 785–796.

[34] K. László, Characterization and adsorption properties of polymer based microporous carbons with different surface chemistry, Microp. Mesop. Mater. 80 (2005) 205–211.

[35] P.-X. Hou, T. Orikasa, T. Yamazaki, K. Matsuoka, A. Tomita, N. Setoyama, Y. Fukushima, T. Kyotani, Synthesis of nitrogen-containing microporous carbon with a highly ordered structure and effect of nitrogen doping on H_2O adsorption, Chem. Mater. 17 (2005) 5187–5193.

[36] C.M. Yang, K. Kaneko, Adsorption properties of nitrogen-alloyed activated carbon fibers, Carbon 39 (2001) 1075–1082.

[37] L. Cossarutto, T. Zimny, J. Kaczmarczyk, T. Siemieniwska, J. Bimer, J.V. Weber, Transport and sorption of water vapour in activated carbons, Carbon 39 (2001) 2339–2346.

[38] M. Seredych, M. Khine, T.J. Bandosz, Enhancement in dibenzothiophene reactive adsorption from liquid fuel via incorporation of sulfur heteroatoms into the nanoporous carbon matrix, ChemSusChem 4 (2011) 139–147.

[39] M. Sevilla, A.B. Fuertes, Sustainable porous carbons with a superior performance for CO_2 capture, Energy Environ. Sci. 4 (2011) 1765–1771.

[40] V. Presser, J. McDonough, S.-H. Yeon, Y. Gogotsi, Effect of pore size on carbon dioxide sorption by carbide derived carbon, Energy Environ. Sci. 4 (2011) 3059–3066.

[41] M.E. Casco, M. Martínez-Escandell, J. Silvestre-Albero, F. Rodríguez-Reinoso, Effect of the porous structure in carbon materials for CO_2 capture at atmospheric and high-pressure, Carbon 67 (2014) 230–235.

[42] K.R. Matranga, A.L. Myers, E.D. Glandt, Storage of natural gas by adsorption on activated carbon, Chem. Eng. Sci. 47 (1992) 1569–1579.

[43] R.F. Cracknell, P. Gordon, K.E. Gubbins, Influence of pore geometry on the design of microporous materials for methane storage, J. Phys Chem. 97 (1993) 494–499.

[44] J.W.F. To, J. He, J. Mei, R. Haghpanah, Z. Chen, T. Kurosawa, S. Chen, W.-G. Bae, L. Pan, J.B.-H. Tok, J. Wilcox, Z. Bao, Hierarchical N-doped carbon as CO_2 adsorbent with high CO_2 selectivity from rationally designed polypyrrole precursor, J. Am. Chem. Soc. 138 (2016) 1001–1009.

[45] Y. Xia, Y. Zhu, Y. Tang, Preparation of sulfur-doped microporous carbons for the storage of hydrogen and carbon dioxide, Carbon 50 (2012) 5543–5553.

[46] N. López-Salas, M.L. Ferrer, M.C. Gutiérrez, J.L.G. Fierro, C. Cuadrado-Collados, J. Gandara-Loe, J. Silvestre-Albero, F. del Monte, Hydrogen-bond supramolecular hydrogels as efficient precursors in the preparation of freestanding 3D carbonaceous architectures containing BCNO nanocrystals and exhibiting a high CO2/CH4 adsorption ratio, Carbon 134 (2018) 470–479.